Precision Measurements of Electroproduction of π^0 near Threshold: A Test of Chiral QCD Dynamics

A Commissioning Experiment for the BigBite Spectrometer

D. Crabb, D. Day, R. Lindgren (spokesperson) [1], B.E. Norum, O. Rondon-Aramayo, B. Sawatzky, K. Wang

University of Virginia, Charlottesville, VA 22903, USA

W. Bertozzi, S. Gilad, D.W. Higinbotham (spokesperson), S. Sirca, R. Suleiman, Z. Zhou

Massachusetts Institute of Technology, Cambridge, MA 02139, USA

J.R.M. Annand (spokesperson), D. Ireland, J. Kellie, K. Livingston, G. Rosner, D. Watts

University of Glasgow, Glasgow, Scotland, UK

V. Nelyubin (spokesperson) [2]

St. Petersburg Nuclear Physics Institute, Gatchina, Russia

D. Margaziotis

California State University, Los Angeles, CA 90032, USA

I.I. Strakovsky, R.A. Arndt, W.J. Briscoe, R.L. Workman

The George Washington University, Washington, DC 20052, USA

Ulf-G. Meißner

Forschungszentrum Jülich Institut für Kernphysik, D-52425 Jülich, Germany

J.P. Chen, C.W. de Jager, R. Michaels, A. Saha, B. Wojtsekhowski

Jefferson Lab, Newport News, VA 22606, USA

J. Goity

Hampton University, Hampton, VA 23668, USA

L. Bimbot

Institut de Physique Nucleaire, F-91406 Orsay Cedex, France

K.G. Fissum

University of Lund, Box 118, SE-221 00 Lund, Sweden

I.A. Rachek [3]

Budker Institute, Novosibirsk, Russia

X. Jiang, R. Ransome

Rutgers University, New Brunswick, NJ 08903, USA

T.R. Hemmert

Technische Universitaet Muenchen, D-85747 Garching, Germany

E. Piasetzky

Tel Aviv, Israel

K. Egiyan, E. Hoohauneysan, A. Keitikyan, S. Mialyan, A. Petrosyan, A. Shahinyan, H. Voskanyan,

Yerevan Physcis Institute

and

The Hall-A Collaboration

Abstract

We propose to make a high precision measurement of the reaction p(e,e'p)π^0 near threshold in a fine grid of Q^2 and ΔW in the range of 0.04 $[GeV/c]^2 \leq Q^2 \leq 0.22$ $[GeV/c]^2$ and 0 $MeV \leq \Delta W \leq 20$ MeV. The experiment will be performed in Hall-A using an HRS spectrometer in coincidence with the large acceptance BigBite spectrometer. The large acceptance of the BigBite spectrometer will enable us to make all measurements with the spectrometers at a single position, thereby minimizing systematic uncertainties. The structure functions $\sigma_T+\epsilon_L\sigma_L$, σ_{TL}, and σ_{TT} will be extracted using the ϕ dependence of the differential cross sections. The results will provide a stringent experimental test of chiral QCD dynamics, a test made all the more critical by recent measurements showing disagreement with the predictions of Chiral Perturbation Theory. The results will be subjected to a full partial wave analysis.

Contents

[1] contact person: R.A. Lindgren, phone: 804-982-2691, e-mail: lindgren@jlab.org

[2] supported by Jefferson Lab and the University of Virginia
[3] supported by Jefferson Lab

1 Introduction

During the last several years significant progress has been made in the application of QCD in the non-perturbative regime via the use of Chiral Perturbation Theory (ChPT). Applied to the π-N system, it starts with a Lagrangian embodying the underlying symmetries of QCD expressed in terms of the relevant degrees of freedom: the pion and the nucleon. Symmetry breaking effects are introduced via perturbative expansions in terms of static and dynamic variables such as m_π/M and Q^2/M, where m_π (M) is the mass of the pion (nucleon) and Q^2 is the four-momentum transferred to the π-N system. Since it involves the well understood electromagnetic interaction and small kinematic quantities, near-threshold electromagnetic production of pions (in particular, neutral pions due to the absence of the overshadowing Kroll-Ruderman term) from nucleons provides an ideal testing ground for ChPT. As ChPT is an "effective" field theory, the description of pion electroproduction contains parameters which must be fixed by measurement, the so-called Low Energy Constants or LEC's. However, once these are fixed it should be possible to predict consistently the evolution with Q^2 and W (center-of-mass energy of the π-N system) of all observables.

Considerable effort has gone into measurements of both the photo-production $p\,(\gamma,\pi^0)$ and electro-production $p(e,e'p)\pi^0$ of neutral pions near threshold. Measurements at Mainz [1] and Saskatoon [2] of the lowest contributing multipole (E_{0+}) to photoproduction are well reproduced by ChPT. The most recent high precision measurements of electroproduction were made at Mainz with four-momentum transfers of 0.10 $[GeV/c]^2$ [3] and 0.05 $[GeV/c]^2$ [4]. The former measurement yielded results consistent with the predictions of ChPT so it was surprising that the latter measurements disagreed significantly. Discrepancies were observed both at threshold (the limiting value of the L_{0+} multipole was observed to be twice the predicted value) and at higher values of W where the P–wave contributions are significant. If these discrepancies which, incidentally, are also inconsistent with the predictions of the SAID analysis and MAID model [5,6], remain unresolved they will constitute a serious threat to the viability of ChPT as a useful theory of dynamical processes. Such a result would be problematical as ChPT is firmly grounded in the basic properties of QCD.

The goal of the proposed measurements is, therefore, to measure precisely the reaction $p(e,e'p)\pi^0$ from threshold to ΔW = 20 MeV above threshold for a range of momentum transfers encompassing those of the Mainz data and extending to both lower and higher values: 0.04 $[GeV/c]^2 \leq Q^2 \leq 0.22[GeV/c]^2$. These data will enable us to a) either confirm or refute the existence of a significant discrepancy with the predictions of ChPT and b) depending upon the result of a) either investigate the source of the discrepancy or test the ability of ChPT to predict higher P–wave contributions.

Hall A of Jefferson Lab provides the foremost facility capable of providing the necessary precision and degree of detail.

The experimental equipment in Hall-A includes the large acceptance BigBite spectrometer [7,8], the High Resolution Spectrometers (LHRS and RHRS) with septum magnets (constructed for experiments [9–11]), and the highly segmented lead glass calorimeter (constructed for experiment [12]). The BigBite spectrometer's 96 msr solid angle acceptance and 80% momentum acceptance will allow new measurements to be made with high statistical precision (1% at peak cross sections). Systematic errors will be minimized since the BigBite spectrometer can measure the entire proton angular distribution within a single kinematic setting. This differs greatly from previous Mainz measurements, where several spectrometer positions were required to cover the necessary angular range. The septum magnet will allow the Hall-A spectrometers to reach small scattering angles (6 degrees) with high beam energies to maximize the cross section for a given Q^2. The lead glass calorimeter will provide a tool to calibrate the acceptance of BigBite.

This combination of equipment, together with the standard equipment in Hall-A, allows neutral pion electro-production cross sections to be measured near threshold on a fine grid of four momentum transfer and pion momentum and angle in the pion-nucleon center of mass system. The measurements proposed herein will cover the four momentum transfer range $Q^2 = 0.04$ - 0.22 $[GeV/c]^2$ and the invariant mass range $\Delta W = 0 - 20$ MeV above threshold. The ϕ dependence of the cross section will be used to extract the structure functions $\sigma_T + \epsilon_L \sigma_L$, σ_{TL}, and σ_{TT}. The cross section data will also be used in a partial wave analysis to provide information on the non-resonant contribution.

In preparation for this experiment, the BigBite spectrometer will be upgraded and commissioned. This will allow it to become a standard piece of Hall-A equipment.

2 Motivation

2.1 Theory

Quantum Chromodynamics (QCD) is the fundamental theory of strong interactions which describes the hadron-hadron interaction in terms of the underlying dynamics of the quark-gluon degrees of freedom. The dynamics of the pion-nucleon system in the low energy regime are largely constrained by chiral symmetry. At low Q^2 and small W, the behavior of the amplitudes can be rigorously determined within ChPT in terms of the perturbative expansions mentioned above. One important issue that can only be answered through the analysis of precise, near-threshold measurements is that of the convergence of the chiral expansion. Such measurements allow one to determine the Low Energy Constants and, consequently, the size of the pion loop contributions. Requiring that the ChPT formalism with a small number of LEC's reproduce data spanning a broad range of kinematic conditions will constitute a crucial test of its predictive power. Examination of existing threshold electro- and photo-production data shows that progress is being made, but that serious inconsistencies remain. Some of these puzzles [13] are discussed below.

2.1.1 S–Wave Amplitudes

In the near threshold regime neutral pion production is dominated by the S–wave amplitudes E_{0+} and L_{0+}; at threshold these are all that survive. These amplitudes combine to give a "reduced" S–wave cross section of $a_0 = |E_{0+}|^2 + \epsilon_L |L_{0+}|^2$ where $\epsilon_L = \frac{Q^2}{\omega_\gamma^2}\epsilon$. The calculated reduced S–wave cross sections a_0 [14,15], shown in Fig. 1, are in fair agreement with world data, but with so few data points and large error bars ($\pm 25\%$), this is not a convincing test of the success or failure of a fundamental QCD theory.

Furthermore, recent studies of the W-dependence of p(e,e'p)π^0 at Mainz for Q^2 =0.05 [GeV/c]^2 [4] and $Q^2 = 0.1[GeV/c]^2$ [3] indicate some inconsistency with ChPT predictions. In these studies, data taken at $Q^2 = 0.10[GeV/c]^2$ were used to determine the LEC's. Using these values, predictions were made for the values of the amplitudes at $Q^2 = 0.05[GeV/c]^2$. At this momentum transfer the transverse S–wave amplitude E_{0+} was observed to be consistent with the prediction ChPT while the longitudinal L_{0+} amplitude exceeded the prediction by about a factor of 2. It is to be noted that in this comparison, ChPT calculations were used to subtract the P–wave contributions. While not very important right at threshold, this subtraction is large for values of W of even a few MeV.

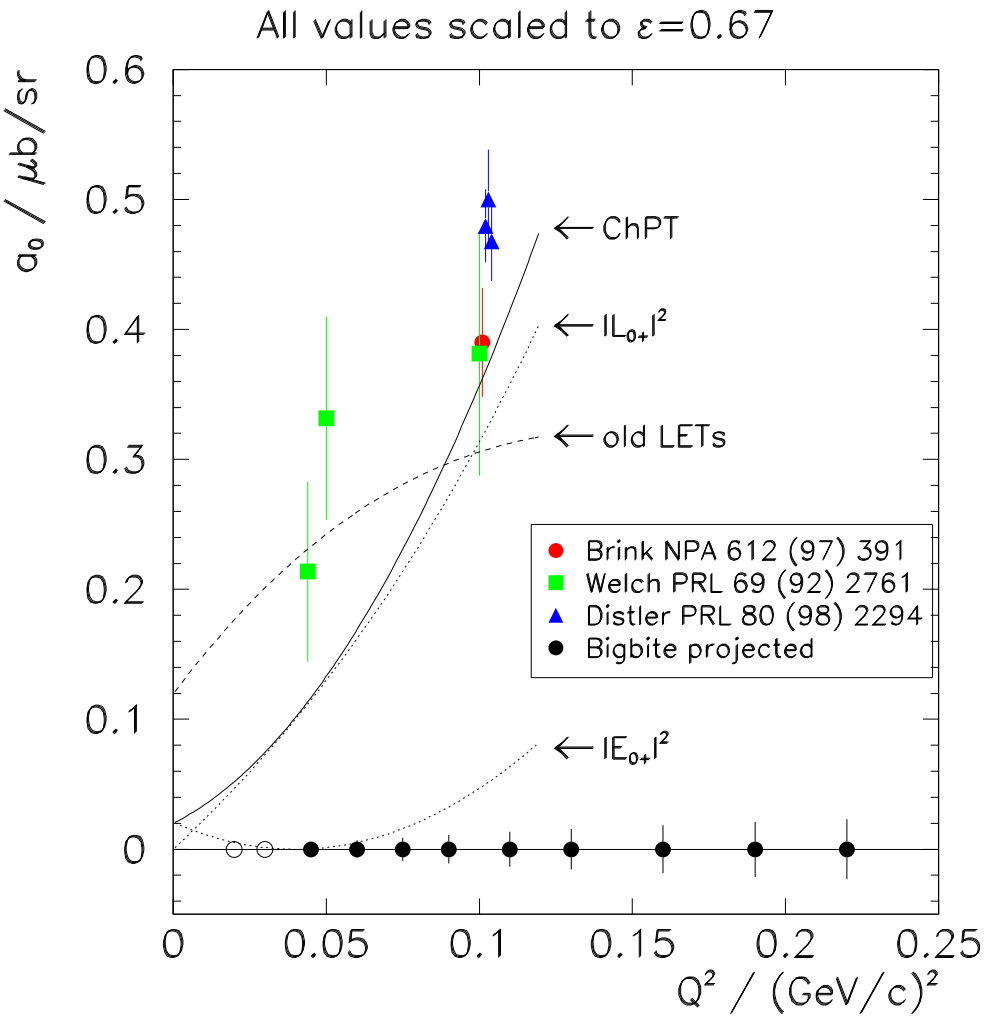

Fig. 1. The S–wave cross section a_0 compared to a_0 extracted from the data for various photon polarizations. The solid line shows the result of a ChPT calculation which used the Distler data to determine the low energy constants. The dotted lines show the E_{0+} and L_{0+} contributions to the cross section. Also shown is a dashed curve showing the result of the old low energy therums. The solid circles show the expected absolute size of the errors of the measures proposed herein. The open circles show the possible data that could be taken at JLAB using a gas target.

2.1.2 P–Wave Amplitudes

In 1996 Bernard [16] pointed out that because the calculated S–wave E_{0+} is a slowly converging function of m_π/M, the ratio of pion to nucleon mass, it is not a very good observable with which to test ChPT at its present level. Until one is confident that the computation of an amplitude has converged, it is not clear what one learns by a comparison with data. In contrast, the calculations of the P–wave multipoles converge much more rapidly. In the low energy expansion, these multipoles have been calculated to next-to-leading order. This makes them much more attractive for tests of ChPT. There are five P-wave multipoles, namely, E_{1+}, two $M_{1\pm}$, and two $L_{1\pm}$. In both the MAMI and NIKHEF analyses for $Q^2 = 0.1$ (GeV/c)^2, they used the P-wave LETs of Ref.[17] to constrain the data. Using these LETS to predict the MAMI data [4] at $Q^2 = 0.05$ (GeV/c)^2, Fig. 2 shows that the extracted transverse-longitudinal interference σ_{LT} term is in poor agreement with these ChPT predictions. The disagreement gets progressively worse from 1.0 to 4.0 MeV above threshold as the expected contribution from P-waves gets bigger suggesting that the P-waves are not yet correctly predicted by ChPT. A similar disagreement is also true for the transverse plus longitudinal cross section. Further evidence[4] that pion electroproduction is not well understood comes from neutral pion production off deuterium at $Q^2 = 0.1(GeV/c)^2$. These large disagreements between the data and ChPT predictions indicate that either we don't understand ChPT as well as we think we do or, perhaps, the data has larger uncertainties than expected. These disagreements are a serious failure of ChPT and should be further investigated from both the theoretical and the experimental sides.

Therefore, to have a better understanding of the S– and P–wave contributions to the cross sections, it is absolutely mandatory to have more precise data in the threshold region, i.e. for energies $0 \leq \Delta W \leq 20$ MeV and on a much finer grid of photon virtualities in the range $0 \geq Q^2 \leq 0.1$ (GeV/c)^2. This will ultimately deepen our understanding of QCD in the non–perturbative regime [13].

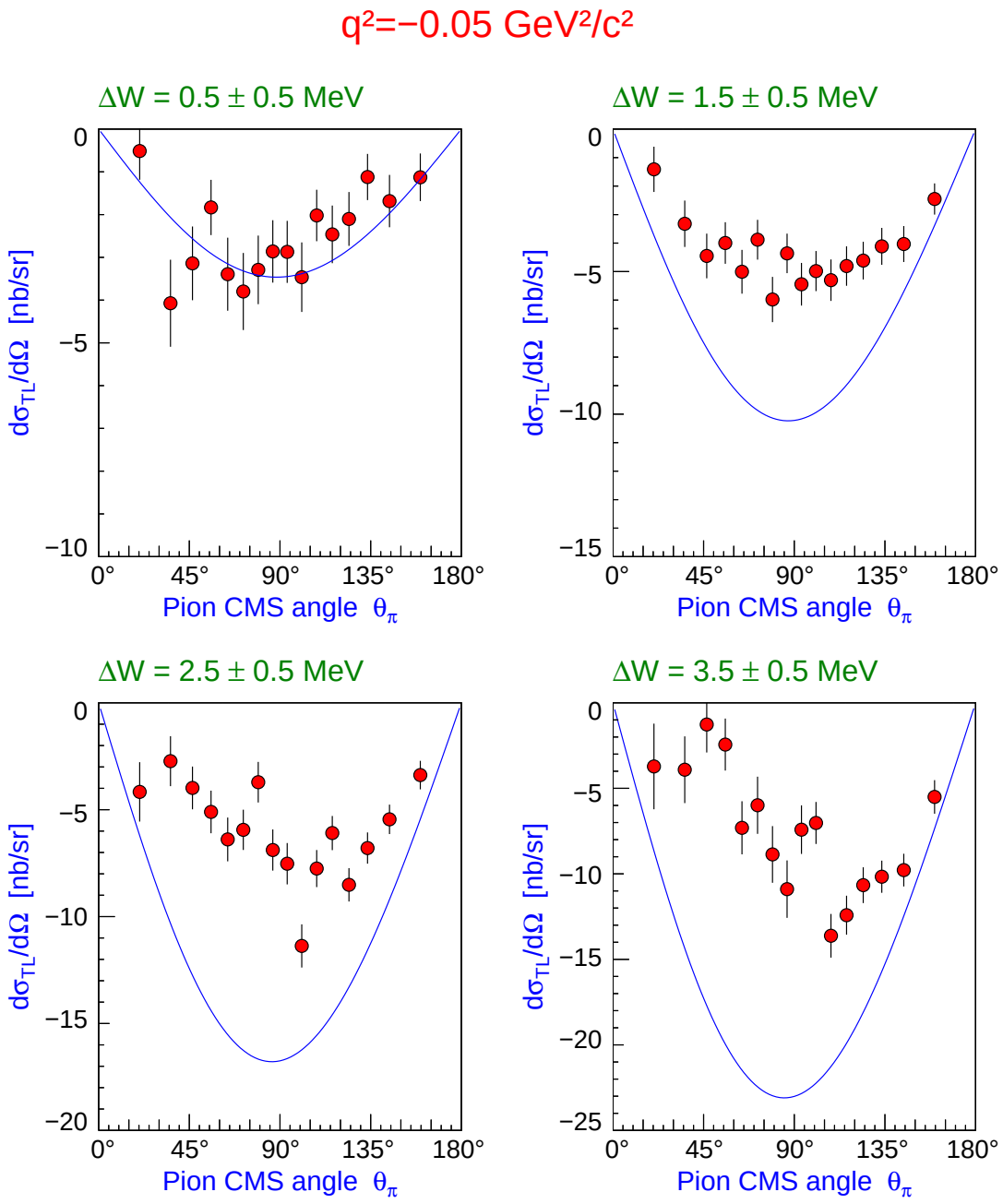

Fig. 2. Shown are the most recent results from Mainz [4]. These results show a large deviation from ChPT predictions. The proposed Hall-A experiment will measure these data to 3% accuracy. The solid lines are predictions of Ref [14].

2.1.3 Partial Wave Analysis

In a partial wave analysis, as performed in the SAID [5] and MAID [6] calculations, the cross section is written as an expansion in six helicity amplitudes [18,6]. Each amplitude is given in a partial wave expansion of products of the electric ($E_{l\pm}$), magnetic ($M_{l\pm}$), and longitudinal ($L_{l\pm}$) multipole amplitudes and the derivatives of Legendre polynomials, where l is the relative pion-nucleon angular momentum and $j = l \pm \frac{1}{2}$ is the total angular momentum. The production amplitudes are determined by fits to the data. The two main sources of experimental data near threshold are from NIKHEF [19] and MAMI [3].

In Fig. 3, the MAMI 1998 differential cross-section data are shown [3] vs. the pion center of mass angle and are compared to the SAID [5] and MAID [6] predictions. Clearly, the data are not fit well by either calculation. Moreover, there appears to be a dip at forward angles that is not predicted by any calculation. Adjustments to the pion multipole amplitudes as shown in Fig. 4 are not sufficient to bring the calculation into agreement with the data. SAID and MAID do not include chiral loops consistently (some through unitarity) and thus it would not be shocking if these failed to work even at $Q^2 = 0.1[GeV/c]^2$. Should these analyses prove unable to accommodate low-Q^2 data, the residual discrepancies could provide information about the chiral loop contributions. However, the current uncertainties are too large to draw any conclusions. Data of much higher precision are required to resolve this apparent discrepancy.

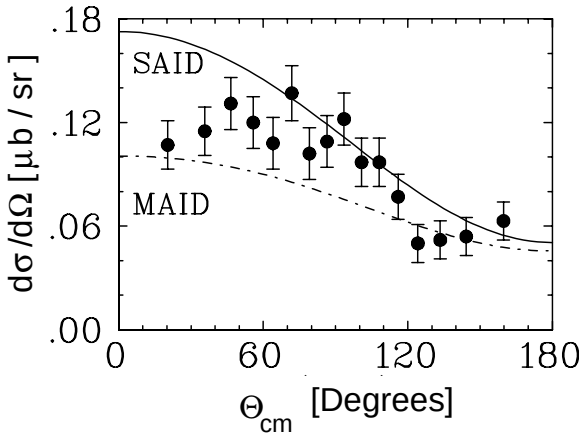

Fig. 3. Shown are the Mainz data [3] taken at Q^2=0.1 [GeV/c]^2 with Δ W = 1 MeV - 2 MeV. The solid and dot-dash curve are the predictions from SAID [5] and MAID [6].

By performing a full partial wave analysis of the data, the various multipole contributions can be determined. As an example, Fig. 4 shows the sensitivity of the cross section, as a function of the center of mass angle of the pion, to the contribution of the P_{33} multipole.

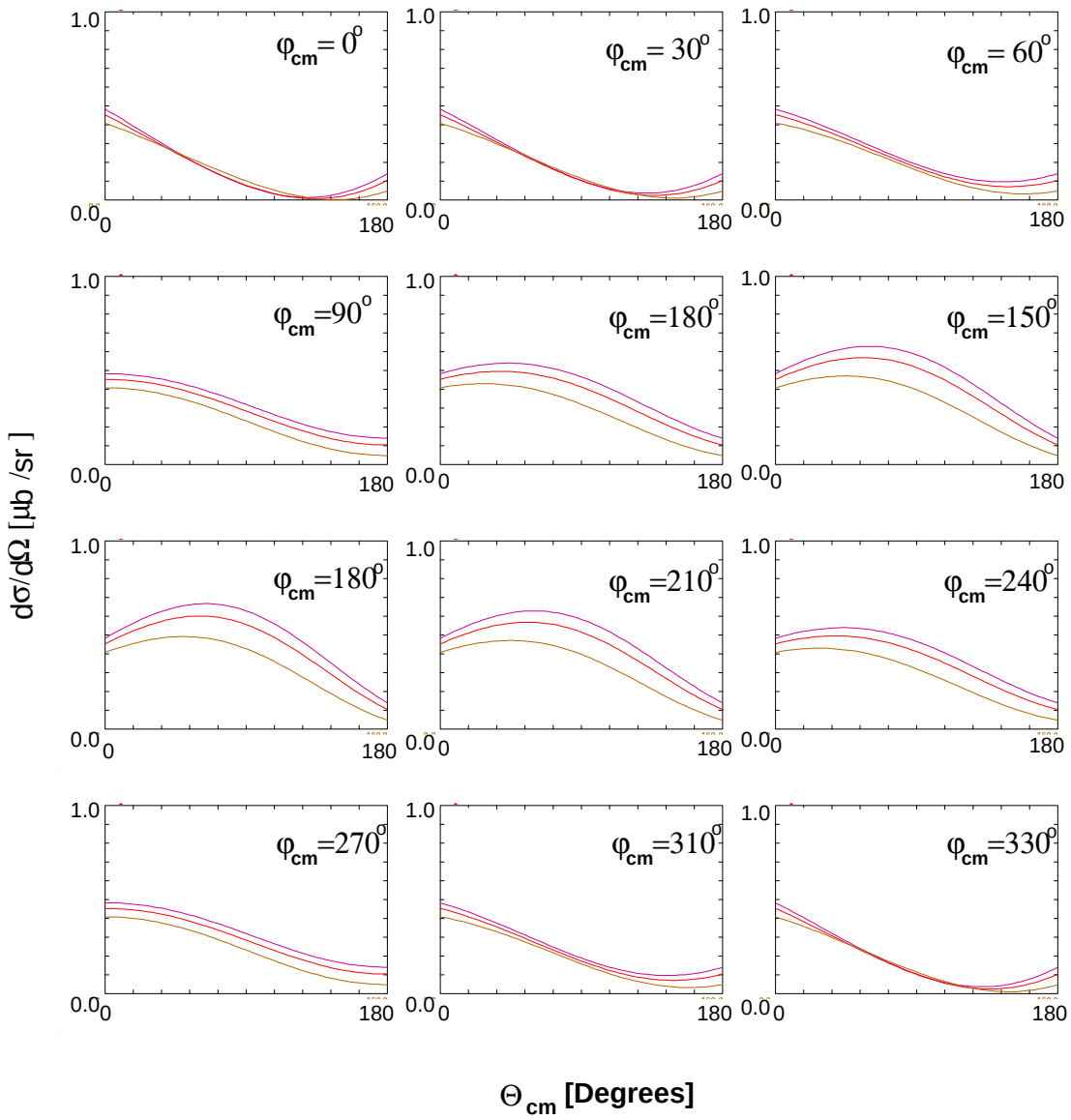

Fig. 4. Shown is the dependence of the differential cross section for a variation in the P_{33} contribution at Δ W = 5 MeV, Q^2=0.1 [GeV/c]^2 as a function of θ_{cm} and ϕ_{cm}. These calculations were produced using SAID [5]. The upper, middle, and lower curves correspond to calculations done by reducing the modulus of the amplitude by 0%, 10% and 30%, respectively.

2.1.4 Review of Previous Experiments

With the availability of high-duty-cycle, medium energy electron accelerators, some progress has been made in determining near-threshold cross sections during the last decade. The characteristics of several threshold experiments are summarized in Table 1. Measurements of $\gamma + p \to p + \pi^0$ at Mainz [1] and Saskatoon [2] have yielded values of the E_{0+}multipole. Ref. [2] is in good agreement with ChPT and also the SAID database fit [5] and near-threshold cross sections are converging to a consensus value.

Compared to photoproduction, electroproduction of π^0 can, in principle, yield a great deal more information allowing a more detailed comparison with theory. Unpolarized $\gamma^* + p \to p + \pi^0$ differential cross section measurements give four (as opposed to one) structure functions, the E_{0+} and L_{0+} multipoles and the dependence on Q^2. However high-accuracy differential cross section measurements over a broad kinematic range are necessary to provide a meaningful comparison with theory.

Facility	Q^2 [GeV/c]^2	ΔW [MeV]	ϕ	Ref.	Comment
MAMI-B	0.0	0–110	N.A.	[1]	E_{0+}, ChPT
Saskatoon	0.0	3–20	N.A.	[2]	E_{0+}, ChPT
NIKHEF	0.04, 0.1	0–2.5	0	[20]	1% duty cycle
NIKHEF	0.1	1–14	0, 180	[19]	E_{0+}, L_{0+}, ChPT
MAMI-B	0.1	≤ 4	0	[3]	L-T sep., E_{0+}, L_{0+}, ChPT
MAMI-B	0.05	≤ 4	0	[4]	Q^2 dependence ChPT

Table 1
List of threshold $\gamma, \gamma^* + p \to p + \pi^0$ measurements. Q is the four-momentum transfer, ΔW is the energy above threshold and ϕ is the azimuthal angle in degrees.

At NIKHEF, following an experiment on the low duty factor linac [20], $p(e, e'p)\pi^0$ differential cross sections $d\sigma/d\Omega_\pi(\theta_\pi, \phi_\pi, W)$ have been measured [19] at $Q^2 = 0.1$ GeV^2 using a 30% duty cycle beam from the AmPS stretcher ring and two, high-resolution magnetic spectrometers. Close to threshold, the final-state proton is emitted in a narrow cone around $\vec{q}$ and so a relatively large coverage of kinematic space can be achieved even with relatively small acceptance spectrometers. E_{0+} and L_{0+} multipoles were extracted from the θ and ϕ cross-section dependence, assuming P–wave multipole values obtained from theoretical predictions. They estimated a maximum model dependence of 10%. Similar measurements, also at $Q^2 = 0.1$ GeV^2, have been made at the Mainz MAMI-B microtron [3] at a luminosity of $\sim 10^{37}$cm^{-2}s^{-1}, where the proton spectrometer covered all of kinematic space up to $\Delta W = 4$ MeV. In this case, a Rosenbluth separation was made and $d\sigma/d\Omega_\pi(\theta_\pi)$ obtained for T, L, LT and TT components. The systematic uncertainty in this experiment,which arose mainly from uncertainties in the electron beam energy and in the calibration of the electron spectrometer, amounted to around 20% at ΔW$\leq$1 MeV and decreased as ΔW increased. The extracted experimental results for the LT component are shown in Fig. 2.

A variety of pion electro-production experiments on the proton have been approved by

Jefferson Lab PAC. However, these experiments focus on the resonance region and not the threshold region. The CLAS detector of Hall B is limited to $Q^2 > 0.4$ GeV^2, mainly by target thickness, and cannot go much above luminosities of $\sim 10^{34}$cm^{-2}s^{-1}. Experiments at MIT-Bates also focus on the resonance region. There is presently no approved Jefferson Lab experiment to probe the low Q^2 threshold region.

3 Experiment

To study the $p(e, ep')\pi^0$ reaction at threshold, we propose to use the large acceptance BigBite spectrometer, LHRS and RHRS with septum magnets, and a lead-glass calorimeter as shown in Fig. 5. The BigBite spectrometer will be used to detect the proton and the LHRS, preceded by a septum magnet, will be used to detect the electron. The high resolution of the electron spectrometer will allow a precise determination of the W and $\vec{q}$ quantities. The large acceptance of BigBite will permit a large fraction of the cone of forward-emitted protons along $\vec{q}$ to be detected. The Hall-A standard 15 cm long liquid hydrogen target will be replaced by a 10 cm version with thinner windows and walls. The RHRS will be used as a single arm electron detector to monitor the luminosity during the experiment. The lead-glass calorimeter, developed for the $p(\gamma, \gamma)$ experiment[12], will be used as an electron arm in coincidence with BigBite to calibrate the BigBite spectrometer's angular and momentum acceptances.

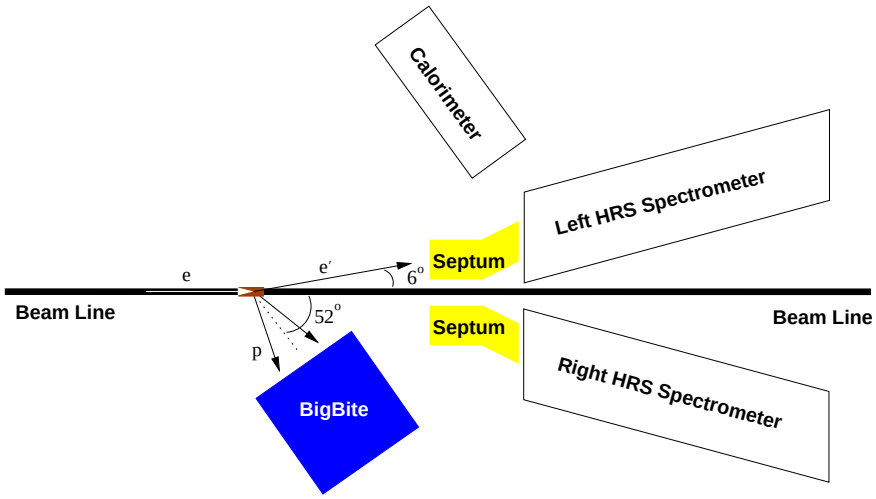

Fig. 5. For the $p(e, e'p)\pi^0$ experiment, the LHRS, RHRS, and the calorimeter will be used as electron detectors and the BigBite spectrometer will be used as a proton detector. The LHRS will be used in coincidence with BigBite for measurement of the $p(e, ep')\pi^0$ reaction. The calorimeter will be used in coincidence with BigBite in order to calibrate the energy and acceptance of the new spectrometer. The RHRS will be used to monitor the luminosity of the experiment. A 10 cm long liquid Hydrogen target will be used.

3.1 Differential Cross Section

The five-fold differential cross section for pion electro-production using an unpolarized electron beam can be written as [21],

$$\frac{d\sigma}{d\Omega_e d\Omega_\pi^* dE'} = \Gamma \frac{d\sigma_v}{d\Omega_\pi^*},$$

where,

$$\frac{d\sigma_v}{d\Omega_\pi^*} = \frac{d\sigma_T}{d\Omega_\pi^*} + \epsilon_L \frac{d\sigma_L}{d\Omega_\pi^*} + [2\epsilon_L(1+\epsilon)]^{1/2} \frac{d\sigma_{TL}}{d\Omega_\pi^*} \cos\phi + \epsilon \frac{d\sigma_{TT}}{d\Omega_\pi^*} \cos 2\phi.$$

A short hand notation for the T, L, TL, and TT two fold differential cross sections in the above formula are σ_T, σ_L, σ_{TL}, and σ_{TT}, respectively. The electron variables are defined in the laboratory system and the pion variables are defined in the pion-nucleon center of mass system designated by *, as shown schematically in Fig. 6. The two-fold differential cross sections (or structure functions) are defined in terms of the pion multipole amplitudes [21], which are functions of the two kinematic variables W, the invariant mass or cm energy of the pion-nucleon system, and the four momentum Q^2. These quantities are defined as,

$$W^2 = -Q^2 + 2m\nu + m^2,$$

$$Q^2 = 4EE' \sin^2 \frac{\theta_e}{2},$$

where m is the proton mass, $\nu = E - E'$, $Q^2 = -q^2$, $q^2 = \nu^2 - |\vec{q}|^2$, θ_e is the electron scattering angle, E is the electron beam energy, and E′ is the scattered electron energy, which is defined as,

$$E' = \frac{E - \frac{W^2 - m^2}{2m}}{1 + \frac{2E}{m} \sin^2 \frac{\theta_e}{2}}.$$

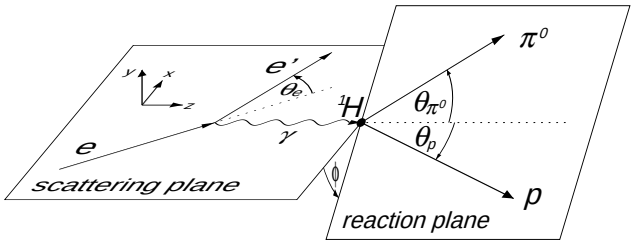

Fig. 6. A schematic of the electron scattering and pion-nucleon reaction plane

The transverse and longitudinal photon polarization parameters, ϵ and ϵ_L, and the virtual flux factor, Γ are defined as,

$$\epsilon = \frac{1}{1 + 2\vec{q}^2/Q^2 \tan^2 \frac{\theta_e}{2}},$$

$$\epsilon_L = \frac{Q^2}{\nu_{cm}^2} \epsilon,$$

$$\Gamma = \frac{\alpha E' k_\gamma}{2\pi^2 E Q^2 (1-\epsilon)},$$

with

$$k_\gamma = \frac{W^2 - m^2}{2m},$$

$$\nu_{cm} = \frac{W^2 - m^2 - Q^2}{2W}.$$

The out of plane ϕ dependence of the cross section will be used to separate and determine the structure functions $\sigma_T + \epsilon_L \sigma_L$, σ_{TT}, and σ_{TL}. Because epsilon is 0.99, the helicity dependent $\sigma_{TL'}$ structure function will not be determined and, therefore, only unpolarized beam will be considered. Threshold measurements will be made as a function of Q^2 and W. The minimum energy, W_{th}, to produce a pion in the CM is $W = m + m_{\pi^0} = 1073.26 MeV$. The CM energy above threshold is denoted by $\Delta W = W - W_{th}$.

3.2 Kinematics

The kinematics of pion production near threshold has the feature that the recoil protons leave the interaction point in a narrow cone in the direction of the virtual photon momentum. The opening angle of this cone depends on W and $\vec{q}$ values. At 1 MeV above threshold, $\Delta W = 1 MeV$, the angle of the cone relative to $\vec{q}$ is about 4° The magnitudes of $\vec{q}$ and W will be determined from the momentum and angle of the scattered electron. Each ring in Fig. 7 beginning at the center corresponds to $\Delta W = 1, 2, 3.., 10 MeV$. In the πN center of mass system the ring corresponds to constant pion momentum and is a function of the pion polar angle from $\theta^*_\pi = 0° - 180°$. The right hand part of the curves corresponds to $\phi_\pi = 0°$ and the left hand part to $\phi_\pi = 180°$. The black lines indicate the acceptance of BigBite in lab proton momentum and lab proton angle. The large vertical angular acceptance of BigBite ($\pm 18°$) allows full coverage of the pion polar CM angle $\Theta^*_\pi = 0° - 180°$ for out of plane angles ϕ near 90° and 270° for $\Delta W = 0 - 20 MeV$. The horozontal angular acceptance of BigBite ($\pm 5°$) allows full coverage of the pion polar CM angle $\Theta^*_\pi = 0° - 180°$ for in plane angles $\phi = 0°$ and 180° for $\Delta W = 0 - 5 MeV$. For other ϕ angles different portions of phase space are covered. In all cases the complete range of proton momenta are obtained.

The measured momentum and the (θ,ϕ) angles of the proton will be used for the calculation of the missing mass and the angles of the pion in the pion-nucleon center of mass system. The missing mass distribution will be used to surpress background. Fig. 8 showns the expected resolution of these quantities as predicted from a GEANT simulation of the BigBite/HRS system.

Near threshold the data will be obtained in 1 MeV bins in ΔW from $\Delta W = 0 - 20 MeV$, and three 0.01 $(GeV/c)^2$ bins in Q^2 for each kinematic setting. The angular distribution for each ΔW and Q^2 bin will be presented in eighteen bins in θ and twelve bins in ϕ. Statistical uncertainties are expected to be on the level of 1-2% at angles where the cross section is maximum and 2.5% on the average.

The count rate estimates in Table 3 are based on the cross section calculations of MAID and SAID for the kinematics shown in Table 2. These predictions have shown reasonable agreement with cross sections measured at MAINZ and NIKHEF in similar kinematics.

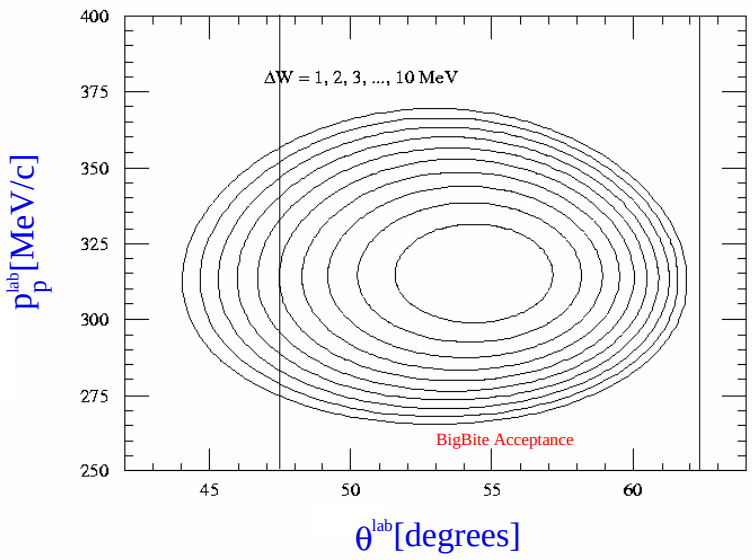

Fig. 7. The momentum of the emitted proton is plotted vs. the scattering angle in the lab for different values of ΔW for $Q^2 = 0.1$ $[GeV/c]^2$. The kinematic region which can be completely measured with a single setting of BigBite with a 10 cm extended target is indicated by the black lines.

Setting Number	E [MeV]	Q^2 $[MeV/c]^2$	W [MeV]	P_p [MeV/c]	Θ_p [degrees]
1	2400	0.04 - 0.08	1074	215 - 275	45 - 54
2	3200	0.07 - 0.14	1074	270 - 340	50 - 57
3	4000	0.11 - 0.22	1074	325 - 430	55 - 59

Table 2
Proposed kinematic settings showing the ranges in P_p and Θ_p for a fixed invariant mass W of 1074 MeV. The BigBite spectrometer does not need to be moved to accommodate these kinematic ranges. The calculations were done for the standard Jefferson Lab beam energies.

Setting Number	Beam Energy [MeV]	HRS Momentum [MeV]	HRS Angle [degrees]	BigBite Momentum [MeV]	BigBite Angle [degrees]	Beam Time [hours]
1	2400	2222	6.0	245	52.0	216
2	3200	2996	6.0	305	52.0	200
3	4000	3769	6.0	378	52.0	192

Table 3
This beam time table assumes a luminosity of 1×10^{37} Hz/cm^2. These settings will cover a Q^2 range of 0.04 - 0.22 $[GeV/c]^2$ and most of phase space for $\Delta W = 0 - 20$ MeV, and some portion of phase space for ΔW up to 200 MeV. One position of the BigBite spectrometer will have sufficient acceptance to perform all three measurements. The estimated beam time assumes that we will obtain 2.5% statistics in each of 54 bins near threshold. Above threshold, the count rate will be higher and allow a finer binning of the data.

Thus, they are considered a realistic estimate of the cross sections. A luminosity of 1×10^{37} Hz/cm^2 is assumed, corresponds to a beam current of 5 uA and a target thickness of

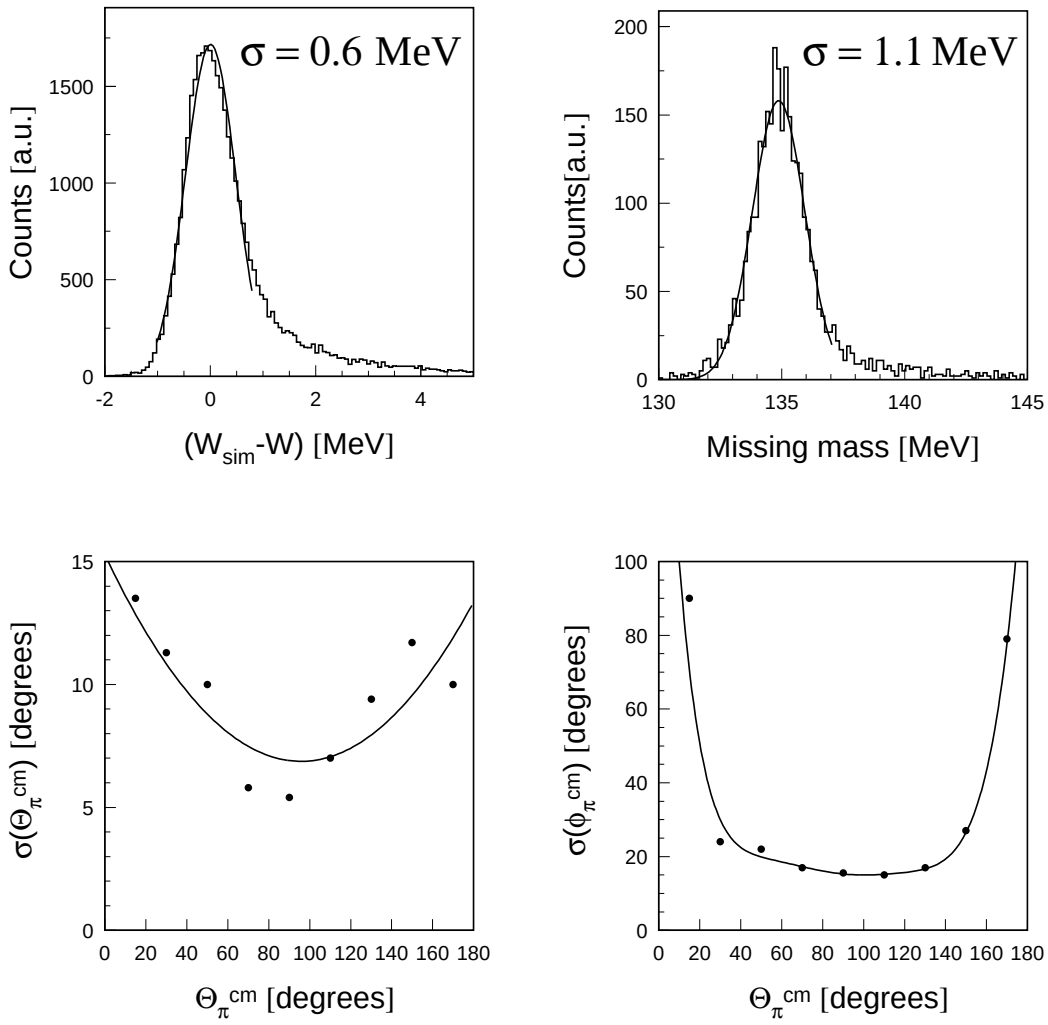

Fig. 8. Shown above is the expected missing mass resolution, the invariant mass W resolution, and the angular resolution of the center of mass angles θ and ϕ. These results were generated using a GEANT Monte Carlo of the BigBite/HRS system.

0.7 gm/cm^2.

3.3 Calibration of the Momentum and Angular Acceptance

The optical properties of the BigBite spectrometer were originally determined at the Internal Target Facility of the AmPS ring at NIKHEF [7,8]. Since then, the spectrometer was disassembled and shipped to Jefferson LAB. UVa and Hall-A have assembled portions of the detector system and have conducted tests of the wire chambers and scintillators using cosmic rays. To take advantage of the luminosity in Hall-A, we plan to upgrade the

detector system to improve its counting capability.

For the calibration, a 1 GeV beam will be used with a highly segmented lead-glass calorimeter to detect electrons scattered through 37°. Because of the target displacement from the pivot point of the HRS due to the septum magnet, the LHRS can not be conveniently used to calibrate BigBite. The calorimeter has excellent angular resolution and can be accurately positioned so that recoil protons scattered into BigBite will have known angles. Recoil protons will typically have scattering angles around 55° and momenta around 600 MeV/c. Variation of beam energy and scattering angle allows us to cover the momentum range of the proposed experiment. Further details of the commissioning of the BigBite spectrometer are discussed in Appendix B.

3.4 Luminosity Measurement

The target thickness-beam current product will be determined with accuracy of about 1-2 % by measuring elastic scattering. This accuracy is sufficient for the proposed experiment. The relative luminosity during the pion production measurements will be monitored in the left RHRS to better than 1%. This technique of using elastic scattering followed by continuous luminosity monitoring has been used by the Hall-A E89044 and E97111 experiments.

3.5 Experimental Equipment

3.5.1 BigBite Spectrometer

The key spectrometer for the proposed experiment is the non-focusing BigBite spectrometer, which has a large solid angle (96 msr) and large momentum acceptance (200-900 MeV/c). A schematic view of BigBite is shown in Fig. A in the Appendix.

The BigBite spectrometer was designed and used at NIKHEF to detect electrons and the angular and momentum resolution was determined with electrons [7,8]. The spectrometer consists of a single dipole magnet followed by a detector system which provides accurate timing (σ=0.75 ns) through use of a fast scintillator, and tracking information by two sets of drift chambers separated by 700 mm. A Cherenkov detector provides discrimination between relativistic and non-relativistic particles. The momentum resolution for the scattered particles is σ=0.84% for 600 MeV/c electrons. The position resolution along the target is σ=3.2 mm, and the angular resolution in both scattering planes is σ=2.3 mrad [7,8]. The two drift chambers have an active area of 1400×350 mm^2 and 2000×500 mm^2, respectively and contain a total of 338 wires and 328 strips. The coordinate in the non-dispersive direction is determined from the measurements of charges induced on three neighboring strips. It is calculated from the center of gravity of these three charges. The coordinate in the dispersive plane is determined from the drift time measurement. The

prompt rate of existing readout electronics for the complete drift chambers is about 27 kHz.

It will be imperative that we conduct this experiment at as high a luminosity as possible to cope with the low cross sections near threshold. At a luminosity of $10^{37} Hz/cm^2$, the total singles rate in BigBite has been calculated using a Monte Carlo simulation based on parasitic experiments, which were conducted in Hall-A under similar conditions using large scintillator arrays. From these measurements and calculations we estimate that the singles rate will be approximately 10^6 Hz which is about 40 times higher than the maximum read out rate for the present wire counters. Plans to upgrade the detectors and readout electronics in BigBite to run at $10^{37} Hz/cm^2$ are given in Appendix A.

In addition to increasing the count rate capability of BigBite, we also intend to improve the angular and momentum resolution by removing all material between the target cell and the detection system of BigBite to reduce straggling and multiple scattering. The vacuum in the scattering chamber will be contiguous with that through BigBite.

A GEANT-based simulation was used to estimate the π^0 angular resolution, the missing mass resolution, and the invariant mass resolution. These results are shown in Fig. 8.

	HRS	BigBite
p-range (MeV/c)	300-4000	200-900
acceptance_H (mr)	± 20	± 80
acceptance_V (mr)	± 60	± 300
solid angle (msr)	4.8	96
Δ p/p	10^{-4}	5×10^{-3}
$\Delta\theta_H$ (mr)	0.6	3.2
$\Delta\theta_V$ (mr)	2.0	3.2
measure	$\vec{p}_e$, vertex	$\vec{p}_p$,vertex
σ_{vertex} (cm)	0.1 (y)	0.32
focusing	$< x\|\theta >= 0$	none
	$< y\|y >= 0$	

Table 4
Comparison of HRS and BigBite.

3.5.2 LHRS arm

The LHRS spectrometer will be used together with a septum magnet to detect electrons at 6°. Its general characteristics are presented in Table 4. To reduce multiple scattering the scattering chamber will be connected directly to vacuum tube of the HRS without any additional window foils. The angular resolution in the horizontal plane is $\sim$ 0.6 mr and in the vertical plane is $\sim$ 2.0 mr. The momentum acceptance is $\pm 4.5\%$ and the angular acceptance in the vertical direction is ± 60 mr and in the horizontal direction is from $+24$ mr to -19 mr. These numbers were used in the Monte Carlo simulation of the missing

mass resolution, the total energy of the $\pi^0 p$-system, and the angular resolution in the CM of this system shown in Fig. 8.

3.5.3 Target Cell

The standard Hall-A, 15 cm long, liquid hydrogen target cell will be replaced by a 10 cm cell with thinner entrance and exit windows and side walls. This is necessary to reduce straggling and multiple scattering for the low energy protons. The existing cryogenic system will be used without modification. Since the beam intensity is about 50 times less than that for the standard target, we can use a target cell with thinner walls. The length of the proposed target cell will be 10 cm with a wall thickness of 10μm of Haval foil. This is important for the small Q^2 region in the proposed experiment. The parameters of target cell are summarized in Table 5.

Hydrogen Density	0.07 gm/cm^3
Cell Length	10.0 cm
Cell Diameter	1.0 cm
Cell Material	Havar Foil
Entrance window	0.001 cm
Exit window	0.001 cm
Side wall	0.001 cm

Table 5
The hydrogen target cell parameters.

In order to possibly extend the measurements of this experiment to Q^2 = 0.02 - 0.04 [GeV/c]^2, we are investigating the possiblity of using a gas target which will further reduce the straggling and multiple scattering.

4 Beamtime Request

We propose an experiment that is a precision test of ChPT. This experiment requires the upgrade and commissioning of the Hall-A BigBite spectrometer. Once commissioned, this spectrometer will be of general utility for future experiments, including a continuation of charged and neutral pion production experiments on the proton and deuteron. As shown in Table 3, 608 hours of beam are needed to complete the three kinematic measurements. Each of the three kinematics will independently provide a complete measurement of the pion electroproduction reaction near threshold. Neither the BigBite spectrometer nor the HRS will need to be moved during these measurements. As shown in Table 6, a total of 35 days is requested to complete both the experimental program and the commissioning of the BigBite spectrometer.

Cross Section Measurements	300 hrs
Energy Changes (2)	15 hrs
Energy Measurements	15 hrs
Subtotal	330 hrs
Calibration Measurements	120 hrs
Energy Changes (2)	15 hrs
Energy Measurements	15 hrs
Subtotal	150 hrs
Total	480 hrs (20 days)

Table 6
Time requested for experiment and commissioning of the BigBite spectrometer.

A Upgrade of BigBite

The BigBite spectrometer will provide a third arm which will greatly extend the experimental capabilities of Hall A. Its large momentum and angular acceptances, which allow a broad kinematic coverage in one setting, will offer completely complementary properties to the high-resolution spectrometers and furthermore will permit the detection of two final-state hadrons.

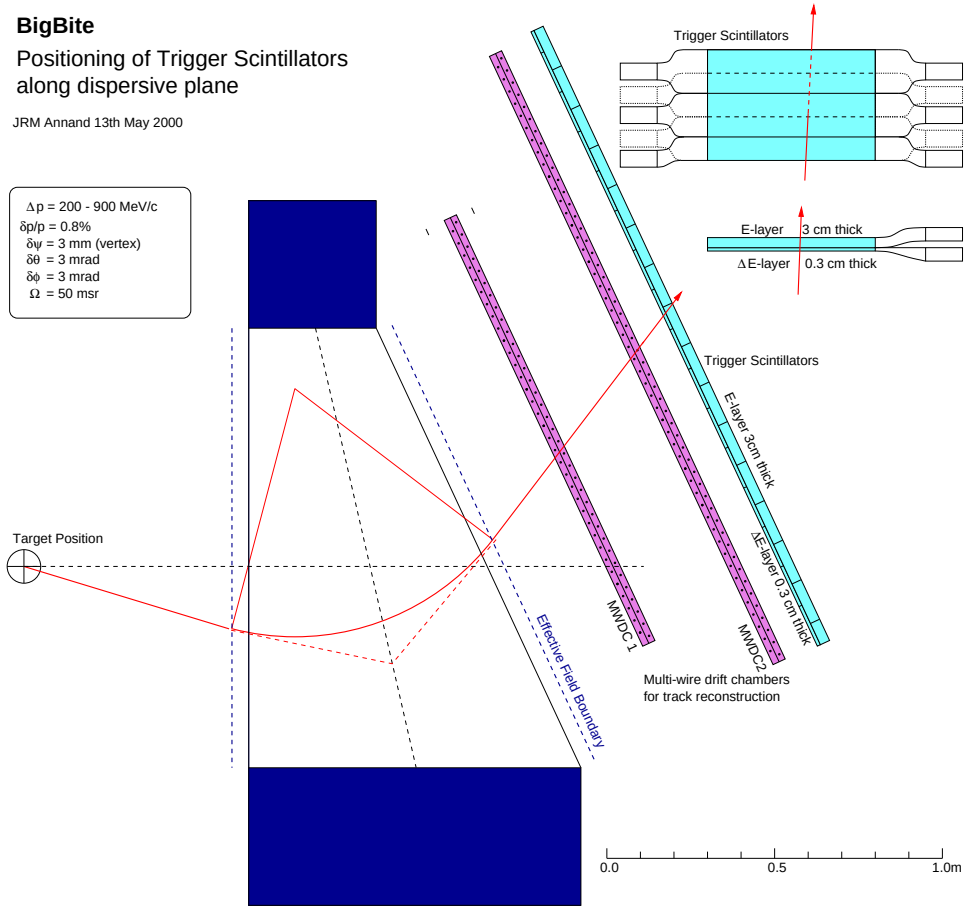

Fig. A.1. Schematic of the BigBite spectrometer showing the trigger scintillator position.

BigBite, originally designed for the low-luminosity NIKHEF internal target facility [7,8], has a 96 msr solid angle, 200–900 MeV/c momentum acceptance and moderate momentum resolution $\sigma_p/p \sim 0.5$ %. In Hall A, luminosities $10^{37} - 10^{38}$ can be achieved and the counting rates in the focal plane detection system will be correspondingly high. For the projected $\gamma^* + p \rightarrow p + \pi^0$ experiment, protons will be ejected from the target at rates $> 10^6$ Hz, necessitating a new focal-plane detection system. It will be necessary to replace both the trigger plastic scintillators and the position sensing multi-wire drift chambers. For proton detection a threshold Cerenkov counter will not be necessary.

Subject to official confirmation, a new trigger detector, to replace the present unsegmented scintillator layer has been funded by the U.K. Engineering and Physical Sciences Research

Council. This detector must provide a precise hit time, to make coincidences with other spectrometers and to reference the multi-wire chambers used for high-precision tracking. Ideally $\sim$0.5 ns FWHM or better is necessary, which is well within the capabilities of plastic scintillator. The geometry of a two-plane system is sketched in Fig. A.1. A coincidence between two planes will provide a very positive hit and $\Delta E/E$ information for particle identification. Each plane will be segmented into 16 elements, each segment being read out via twisted-strip light guides by two, fast 50 mm photomultipliers (PM). Two PM will provide a position-independent mean time, position information in the non-dispersive direction ($\delta y \sim 4$ cm FWHM) via time difference and optimum pulse-height resolution. Staggering the elements of each scintillator layer (Fig. A.1) will give a position resolution in the dispersive direction of $\pm$6.45 cm.

For initial testing the original drift chambers will be used, but it is clear that a MWPC design will be necessary for the experiment proper. Development of this component of the focal plane will take place in parallel with other Hall A projects. The supplemental position information from the trigger detector may by useful to resolve ambiguities in the hit information given by fast-counting wire chambers

Circuitry for time pickoff, coincidence logic, analogue-to-digital conversion and high-voltage generation will be largely implemented in commercial electronics in general medium-energy physics use. Programmable discriminators and logic units will be in the CAMAC standard while QDC's and TDC's will be VMEbus. Instrumentation of the MWPC will be in the standard LeCroy "PCOS 4" system. Due to the expected rates there will no multiplexing.

High rates will place a heavy demand on the data acquisition and we make provision for a dedicated VMEbus based system to handle this task. We are developing software to read out and control both the scintillators and the multi-wire drift chambers, to fit within "CODA" which is the default system at Jefferson Lab. Hand in hand with this effort goes the writing of BigBite momentum reconstruction software, which will be made within the new C++ Hall-A data analysis system, based on CERN "Root".

B Calibration of BigBite

In order to calibrate the large acceptance BigBite spectrometer, the electromagnetic calorimeter, which is being built for experiment E99-114 [12], will be used. The calorimeter will be used to measure the energy and angle of elastically scattered electrons. The calorimeter consists of 32 layers with 22 lead glass modules in each layer totaling 704 modules. The energy and spatial resolution of the scattered electron can be determined with a resolution better than $\sigma_{\delta E/E} = 0.01 + 0.06/\sqrt{E(GeV)}$ and with a spatial resolution of 4.3 mm, respectively.

The calorimeter will be centered at 35° in order to detect elastic electrons in coincidence with recoil protons at 54° in BigBite as shown in Fig. 5. The advantage of this method is the calibration location is the same as the experimental one. Therefore, systematic errors related to moving BigBite are avoided. The large out-of-plane acceptance of BigBite is well matched to the calorimeter's out-of-plane acceptance. Survey of the calorimeter with an acceracy of 1 mm will allow an absolute angular calibration of the BigBite spectrometer to acceracy of 0.2 mr.

The Hall-A multi-foil target will be used to calibrate the reconstruction of the target position of the BigBite spectrometer. The thin CH2 target and the 10 cm liquid targets will be used during the elastic scattering calibration measurements. Due to the large momentum acceptance of the BigBite spectrometer, we will make use of the elastic radiative tail to calibrate the entire momentum acceptance with a minimum number of different beam energies. This calibration will provide the momentum calibration to better than 0.5%, and a recoil angle calibration precision better than 1 mr. The calibrations will be performed at first with the B field field set to zero, which will offer a check of the wire chamber resolution. Then the B field will be turned on to its full value for the momentum calibration. These techniques are similar to those that were developed at NIKHEF to originally commission the BigBite spectrometer [7,8].

Assuming this will be the first experiment to use the BigBite spectrometer in Hall-A, we request 120 hrs of beamtime to commission the spectrometer. We will make use of the 800 MeV and 1600 MeV beams energies during the commissioning.

References

[1] M.Fuchs *et al.*, Phys. Lett. **B368** (1996) 20.

[2] J.C. Bergstrom *et al.*, Phys Rev. **C53** (1996) R1052.

[3] M.O.Distler *et al.*, Phys. Rev. Lett. **80** (1998) 2294.

[4] H. Merkel, Pion threshold electro- and photo- production, Talk for the Chiral Dynamics 2000 Workshop.

[5] R. A. Arndt, I. I. Strakovsky and R. L. Workman, Phys. Rev. **C53** (1996) 430, http://www.gwu.edu/dac/dacstart.html.

[6] D. Drechsel, O. Hanstein, S. S. Kamalov and L. Tiator, Nucl. Phys. **A645** (1999) 145.

[7] D.J.J. de Lange *et al.*, Nucl. Instr. and Meth. **A 406** (1998) 182.

[8] D.J.J. de Lange *et al.*, Nucl. Instr. and Meth. **A 412** (1998) 254.

[9] K. Kumar *et al.*, Constraning the nucleon strangeness radius in parity violating electron scattering, TJNAF Proposal E99-115.

[10] D. Amrstong *et al.*, Parity violation from ^4He at low q^2: A clean measurement of ρ_s, TJNAF Proposal E00-114.

[11] R. Michaels, A clean measurement of the neutron skin of ^{208}Pb through parity violating electron scattering, TJNAF Proposal E00-003.

[12] C. Hyde-Wright *et al.*, Exclusive compton scattering on the proton, TJNAF Proposal E99-114.

[13] U.-G. Meissner, Chiral QCD: Baryon dynamics, in *Encyclopedia of Analytic QCD*, edited by to be published by World Scientific M. Schifman, 2000.

[14] V. Bernard, N. Kaiser and Ulf-G. Meißner, Nucl. Phys. **A607** (1996) 379.

[15] V. Bernard, N. Kaiser and Ulf-G. Meißner, Nucl. Phys. **A633** (1998) 695.

[16] V. Bernard *et al.*, Z. Phys **C70** (1996) 483.

[17] V. Bernard, N. Kaiser and Ulf-G. Meißner, Phys. Rev. Lett. **74** (1995) 3752.

[18] R. A. Arndt, R. L. Workman, Zh. Li and L. D. Roper, Phys. Rev. **C42** (1990) 1853.

[19] H.B. van den Brink *et al.*, Nucl. Phys. **A612** (1997) 391.

[20] T.P. Welch *et al.*, Phys. Rev. Lett. **69** (1992) 2761.

[21] D. Drechsel and L. Tiator, J. Phys. G: Nucl. Part. Phys. **18** (1992) 449.